Heparan sulfate proteoglycans can promote opposite effects on adhesion and directional migration of different cancer cells

Journal:	*Journal of Medicinal Chemistry*
Manuscript ID	jm-2020-01848f.R1
Manuscript Type:	Article
Date Submitted by the Author:	n/a
Complete List of Authors:	Depau, Lorenzo; University of Siena, Medical Biotechnologies Brunetti, Jlenia; University of Siena, Medical Biotechnologies Falciani, Chiara; University of Siena, Medical Biotechnologies Mandarini, Elisabetta; University of Siena, Medical Biotechnologies Riolo, Giulia; University of Siena, Medical Biotechnologies Zanchi, Marta; University of Siena, Medical Biotechnologies Karousou, Evgenia; University of Insubria, Surgery and morphology sciences Passi, Alberto; University of Insubria, Surgery and morphology sciences Pini, Alessandro; University of Siena, Medical Biotechnologies Bracci, Luisa; University of Siena, Medical Biotechnologies

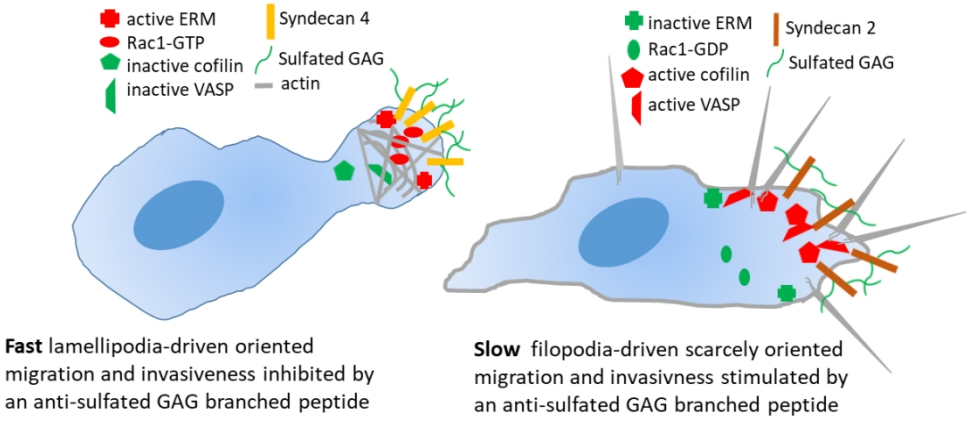

Table of Contents graphic

107x48mm (300 x 300 DPI)

Heparan sulfate proteoglycans can promote opposite effects on adhesion and directional migration of different cancer cells

Lorenzo Depau,[1#] Jlenia Brunetti,[1#] Chiara Falciani,[1] Elisabetta Mandarini,[1] Giulia Riolo,[1] Marta Zanchi,[1] Evgenia Karousou,[2] Alberto Passi,[2] Alessandro Pini[1] and Luisa Bracci[1]*

[1] Department of Medical Biotechnologies, University of Siena, 53100 Siena, Italy

[2] Department of Medicine and Surgery, University of Insubria, 21100 Varese, Italy

# These two authors contributed equally to the paper

Abstract

Heparan sulfate proteoglycans take part in crucial events of cancer progression, such as epithelial mesenchymal transition, cell migration and invasion. Through sulfated groups on their glycosaminoglycan chains, heparan sulfate proteoglycans interact with growth factors, morphogens, chemokines and extracellular matrix proteins. The amount and position of sulfated groups are highly variable, thus allowing differentiated ligand binding and activity of heparan sulfate proteoglycans. This variability and the lack of specific ligands have delayed comprehension of the molecular basis of heparan sulfate proteoglycan functions.

Exploiting a tumor-targeting peptide tool that specifically recognizes sulfated glycosaminoglycans, we analyzed the role of membrane heparan sulfate proteoglycans in adhesion and migration of cancer cell lines. Starting from the observation that the sulfated glycosaminoglycan-specific peptide exerts a different effect on adhesion, migration and invasiveness of different cancer cell lines, we identified and characterized three cell migration phenotypes, where different syndecans are associated to alternative signaling for directional cell migration.

Keywords: Heparan sulfate proteoglycans, cell migration, cytoskeleton, tumor marker, peptide

Introduction

Alterations of glycosaminoglycan (GAG) chains in the so-called glycocalix of cancer cells and the presence of GAG chains in body fluids from cancer patients have been known for decades.[1,2] However, there is accumulating evidence that the role of heparan sulfate proteoglycans (HSPG) in cancer cell biology may have been severely underestimated for years.

HSPGs consist of a core protein carrying O-linked saccharide chains. They may be anchored to the cell membrane or dissolved in the extracellular matrix (ECM). On the basis of their core protein, cell membrane HSPGs can be divided into syndecans, which have a transmembrane protein core with intracellular domains, and glypicans, which have an extracellular glycosylphosphatidylinositol membrane-anchored protein core. The GAG chains of syndecans and glypicans are large, linear, negatively charged polysaccharides, consisting of repeated disaccharide units that can be sulfated at different positions and to different extents, creating great modular variety. GAG chains of membrane HSPGs are mainly heparan sulfate (HS), with chondroitin sulfate (CS) only occurring in a subset of membrane syndecans.[3-5]

The biological functions of HSPGs reside in their ability to interact with various heparin-binding ligands, including growth factors, morphogens, chemokines, adhesion molecules and ECM components. Thanks to their many interactions, HSPGs are known to take part in major cell signaling events that regulate cell proliferation, differentiation and directional migration, both under physiological conditions, like embryo development and tissue regeneration, and under pathological conditions, like cancer.[6]

HSPGs appear to take part in many crucial events of cancer cell differentiation, like epithelial-mesenchymal transition, as well as in cancer cell contacts with surrounding cells and ECM, cell division, migration and invasion.[4-6] Although their role in events regulating cancer cell differentiation

and migration has long been recognized, HSPGs were mainly regarded as coreceptors for growth factors or morphogens and as having an ancillary role in cell adhesion and migration by facilitating the function of integrins.[5] There is now accumulating evidence suggesting a determinant and more autonomous role of HSPGs in cancer-cell signaling.[7-9]

Interactions of HSPGs with their ligands are mainly mediated by GAG chains, with sulfate groups playing a crucial role.[10-12] Similar sulfated GAG chains can be present on different glypicans and syndecans, which can therefore share ligand binding. Nonetheless, different protein cores can result in different signal transmission, since only syndecans have intracellular protein domains that can mediate contact with adaptor proteins or enzymes, and even among syndecans, specific intracellular domains are known to mediate different cell responses.[3-6]

The synthetic and post translational variability of HSPG GAG chains makes it difficult to understand the molecular basis of their activities. Despite much information on the many different functions of HSPGs in physiological and pathological events, the molecular basis of their activities is still far from understood.

In previous papers, we reported the synthesis and biological activity of a tetra-branched peptide, named NT4, which very selectively binds cell lines and tissues of different human cancers, including colon adenocarcinoma, pancreas adenocarcinoma, bladder cancer and breast cancer.[13-15] The selectivity of NT4 peptide can be exploited for cancer imaging and therapy. NT4 coupled to different functional units can efficiently deliver drugs or tracers for cancer cell therapy or imaging.[15-20] Using drug-conjugated NT4, we obtained a significant reduction in tumor growth compared with animals treated with the unconjugated drug under identical conditions.[15,17] Drug-conjugated NT4 can by-pass drug resistance mediated by membrane transporters.[21] Unlike the unconjugated drug, NT4 conjugated to paclitaxel produced tumor regression and even clearance of cancer cells in an orthotropic model of human breast cancer.[22]

We found that the high selectivity of the NT4 peptide towards cancer cells and tissues resides in its high affinity binding to sulfated GAGs, with preferential binding to heparin and heparan sulfate and

no binding to the non-sulfated hyaluronic acid.[23,24] NT4 binding to different cancer cell lines and tissues is abolished by heparin and heparan sulfate and is also inhibited by heparin-binding proteins, like midkine and ApoE. Systematic modification of the amino-acid sequence in the NT4 peptide led to identification of a multimeric positively-charged motif that mediates interaction of NT4 with sulfated GAGs and which is very similar to heparin-binding motives contained in midkine and other proteins, like Wnt, which bind sulfated GAGs and are over-expressed in cancer.[23] Moreover, by using different sulfated oligosaccharides and recombinant HSPGs, we recently demonstrated that the specific binding of NT4 to sulfated GAGs is dependent on the number and position of sulfated groups.[25]

Based on its specific binding to sulfated GAGs, we have been using the peptide NT4 as a tool for decoding the role of HSPGs in cancer cell adhesion and migration. We found that NT4 inhibits adhesion of PANC-1 human pancreas adenocarcinoma cells to collagen, cellular fibronectin and plastic, and dramatically inhibits directional migration of these cancer cells on different supports.[24] Since the use of NT4 as a specific tool allowed us to identify a crucial role of HSPGs in PANC-1 cell adhesion and directional migration, we checked whether the role of HSPGs is shared by different cancer cells by testing the effect of NT4 on adhesion and migration of different cancer cell lines. Despite similar specific binding to the cancer cell membrane, we found that the effect of NT4 on adhesion and migration is extremely variable in different cancer cell lines, indicating that cancer cells can use different molecular mechanisms for adhesion and migration, with different contributions of HSPGs.

We selected three human cancer cell lines on the basis of different effects produced by the sulfated GAG-specific probe NT4 on adhesion and migration: 1) PANC-1 cells, where NT4 inhibits both adhesion and migration; 2) TE671 rhabdomyosarcoma cells, where NT4 does not efficiently inhibit adhesion but increases cell migration; and 3) HT29 cells, where NT4 inhibits adhesion to different supports but the cells do not migrate on solid supports or in transwell migration experiments. To have a complete picture of cell directional migration signaling in the three cell lines, we analyzed

expression of syndecans and glypicans and we studied actin filament organization as well as E- and N-cadherin expression and distribution in the cells under static and migrating conditions. We also analyzed expression of proteins and enzymes involved in molecular signaling regulating cancer cell migration in the three cell lines, evaluating the effect produced by the sulfated GAG-specific ligand NT4. This approach allowed us to identify different cancer cell phenotypes and molecular signaling associated with lamellipodia- or filopodia-driven cell migration, where HSPGs appear to play crucial but diverse roles.

Results

Binding of the peptide NT4 to sulfated GAGs has variable effects on adhesion of different cancer cell lines to solid supports

We selected human cell lines from tumors of different origin, PANC-1 pancreas adenocarcinoma, HT29 colon adenocarcinoma, T24 bladder carcinoma, A375 melanoma, MDA-MB 231 breast adenocarcinoma, MCF7 breast adenocarcinoma and TE671 rhabdomyosarcoma. Using flow cytometry, binding of NT4 peptide to each cell line was tested and specificity was probed by inhibition by heparin of the same binding (Fig. 1a,b). We then tested the effect produced by NT4 on adhesion of the same cell lines to culture plates coated with fibronectin from human fibroblasts (cellular fibronectin), fibronectin from human plasma (plasma fibronectin), collagen IV or to uncoated wells (Fig. 1c-f).

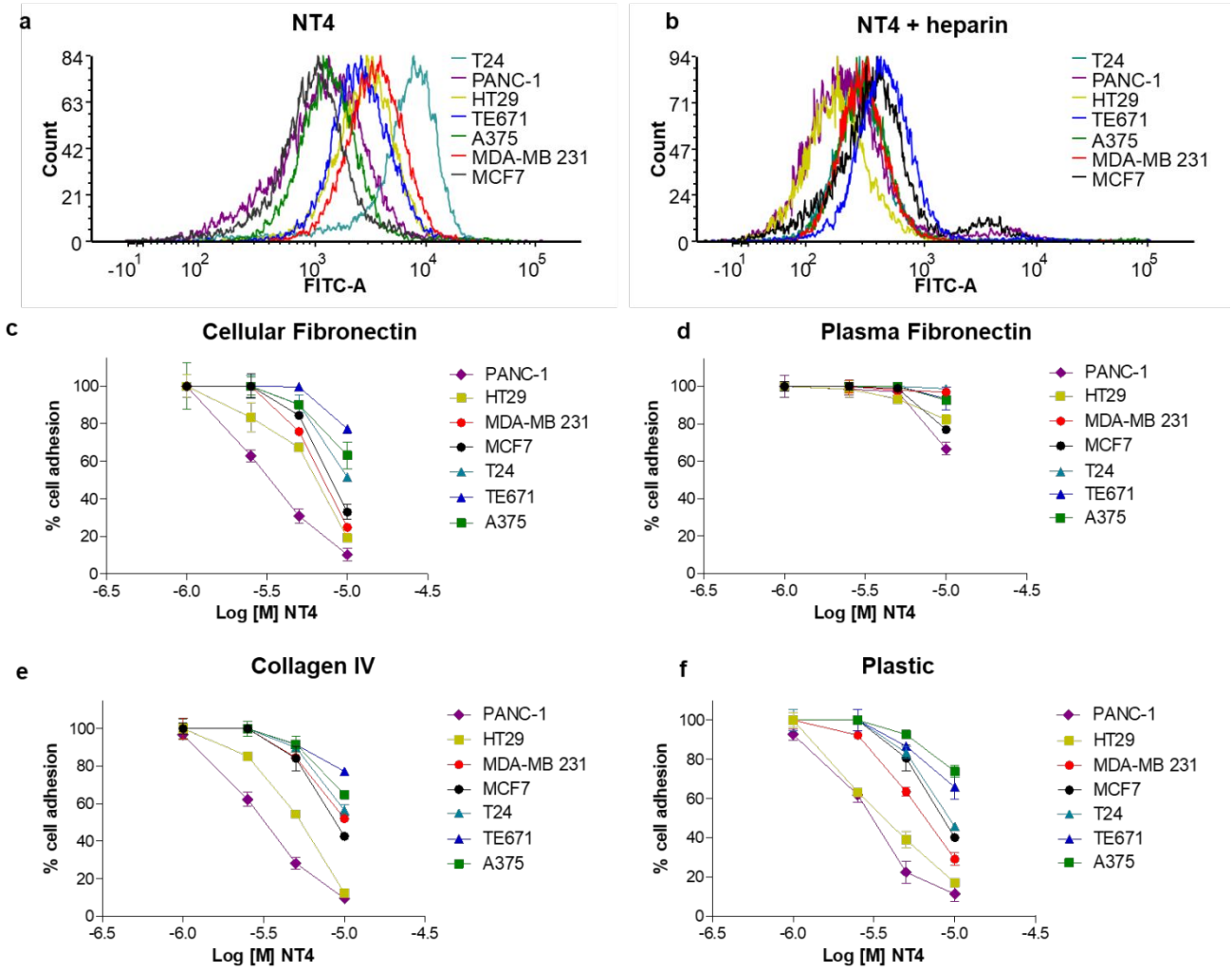

Fig. 1 NT4 specific binding to cancer cells produces different effects on cell adhesion. a) NT4 binding and b) inhibition of NT4 binding by heparin to PANC-1, HT29, MDA-MB 231, MCF7, T24, TE671 and A375 cancer cells, analyzed by flow cytometry. c-f) Adhesion of different human cancer cell lines to cellular fibronectin, plasma fibronectin, collagen IV and plastic at different molar concentrations of NT4. Data are reported as percentage of control cell adhesion (same cell line incubated without NT4 in identical conditions).

Although NT4 specifically bound to all the cancer cell lines, the effect produced by the peptide on cell adhesion was extremely variable. The highest inhibitory effect was obtained on adhesion of PANC-1 cells to all supports, except plasma fibronectin, confirming our previously reported results.[24] Slightly lower inhibition of adhesion was obtained with HT29 cells, whereas inhibition of adhesion by NT4 on other cell lines was much lower. In particular, NT4 was almost ineffective at inhibiting

adhesion of TE671 cells to all supports. Although the cell lines were affected differently by NT4, adhesion to plasma fibronectin was not inhibited by NT4 for any of them.

These results indicate that cancer cell adhesion may be variably modulated by sulfated GAGs. PANC-1 and HT29 cells seem mainly to adhere to different substrates through sulfated GAG chains, whereas TE671 cells seem less dependent on sulfated GAGs for adhesion to different substrates. Adhesion of all the cell lines to plasma fibronectin seems to be independent of sulfated-GAGs. Unlike cellular fibronectin, plasma fibronectin is a minor component of the ECM and does not contain EDA and/or EDB segments which have long been known to be expressed in cancer tissues and whose ligands are reported to be inhibited by heparan sulfate.[26]

Binding of NT4 to sulfated GAGs can either inhibit or stimulate directional migration and invasiveness of different cancer cell lines.

Since the role of HSPGs appeared to be different in adhesion of distinct cancer cells, we reasoned that differences in the control of cell migration may also exist. We then analyzed the effect produced by NT4 on 2D migration in wound healing experiments of PANC-1, TE671 and HT29 cell lines, selected on the basis of the diversified effect produced by the sulfated GAG-specific probe on adhesion to different supports.

Migration of PANC-1 cells was inhibited by NT4 on uncoated plastic wells and on plasma and cellular fibronectin, as demonstrated by wound healing experiments (Fig. 2a and videos supplement S1,2). Untreated TE671 cells seemed to migrate slower than untreated PANC-1 cells, as indicated by the rate of gap filling in the same time interval. In sharp contrast to PANC-1 cells, TE671 cells treated with NT4 peptide filled the gap in a shorter time than untreated cells (Fig. 2b and videos S3,4). HT29 cells did not migrate in wound healing experiments on any support, with or without NT4 (Fig. 2c and videos S5,6).

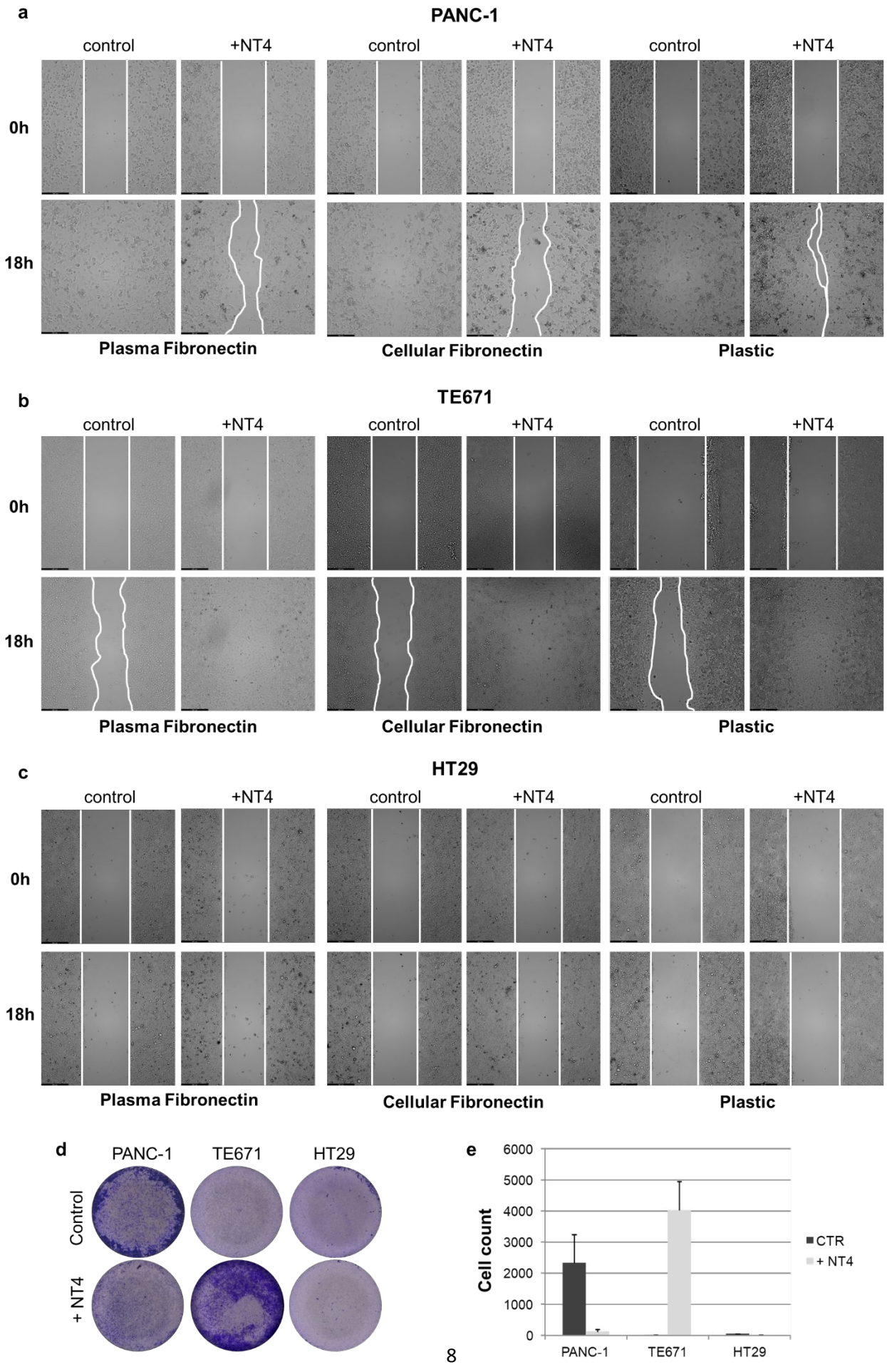
a
PANC-1
control
+NT4
control
+NT4
control
+NT4
0h
18h
Plasma Fibronectin
Cellular Fibronectin
Plastic
b
TE671
control
+NT4
control
+NT4
control
+NT4
0h
18h
Plasma Fibronectin
Cellular Fibronectin
Plastic
c
HT29
control
+NT4
control
+NT4
control
+NT4
0h
18h
Plasma Fibronectin
Cellular Fibronectin
Plastic
d
PANC-1
TE671
HT29
Control
+ NT4
e
Cell count
6000
5000
4000
3000
2000
1000
0
PANC-1
TE671
HT29
CTR
+ NT4

Fig. 2 Migration of cancer cells. a-c) Wound healing assay. PANC-1 (a), TE671 (b) and HT29 (c) cancer cells were plated on wells coated with plasma fibronectin, cellular fibronectin or on uncoated wells where a silicon spacer had been placed immediately before cell plating. Once cells had reached confluence, the silicon spacer was removed and the cells were treated with 10 μM NT4 peptide for 18 hours. Phase-contrast microscopy images were acquired from each well at time 0 (0 h) and 18 hours (18 h) after removal of the silicon spacer. d-e) Invasion assay. d) Image of PANC-1, TE671 and HT29 cancer cells invading the lower well of Boyden chambers. Cells were seeded on the upper part of transwell inserts previously coated with collagen I and incubated for 24 h without NT4 (control) or with 10 μM NT4 (+ NT4). e) Images of migrating cells, fixed and stained with crystal violet, were obtained by confocal microscopy on the entire well surface and ImageJ was used to count cells.

Time lapse analysis of migrating PANC-1 and TE671 cells showed different migration behaviors, even in the untreated control cells (videos S1,3). Untreated PANC-1 cells migrated in an organized directional way on all supports (video S1); lamellipodia were clearly evident and were stable in many of the cells, which generally maintained their direction. Migration of untreated TE671 cells appeared to be less directional; the cells seemed unable to maintain directional migration and lamellipodia were less evident and appeared unsteady compared to untreated PANC-1 cells (video S3). The very different effect produced by the sulfated GAG-specific NT4 peptide on PANC-1 and TE671 cells was confirmed by the time lapse analysis of cell migration (videos S2,4).

In order to compare the different migration behavior of control and treated cells in the two cell lines, we analyzed single cell tracks, measuring both accumulated distance, i.e. the pathway effectively covered by each cell, and Euclidean distance, i.e. the distance between the starting and the arrival point of the same tracks (Fig. supplementary S1 and Fig. 3).

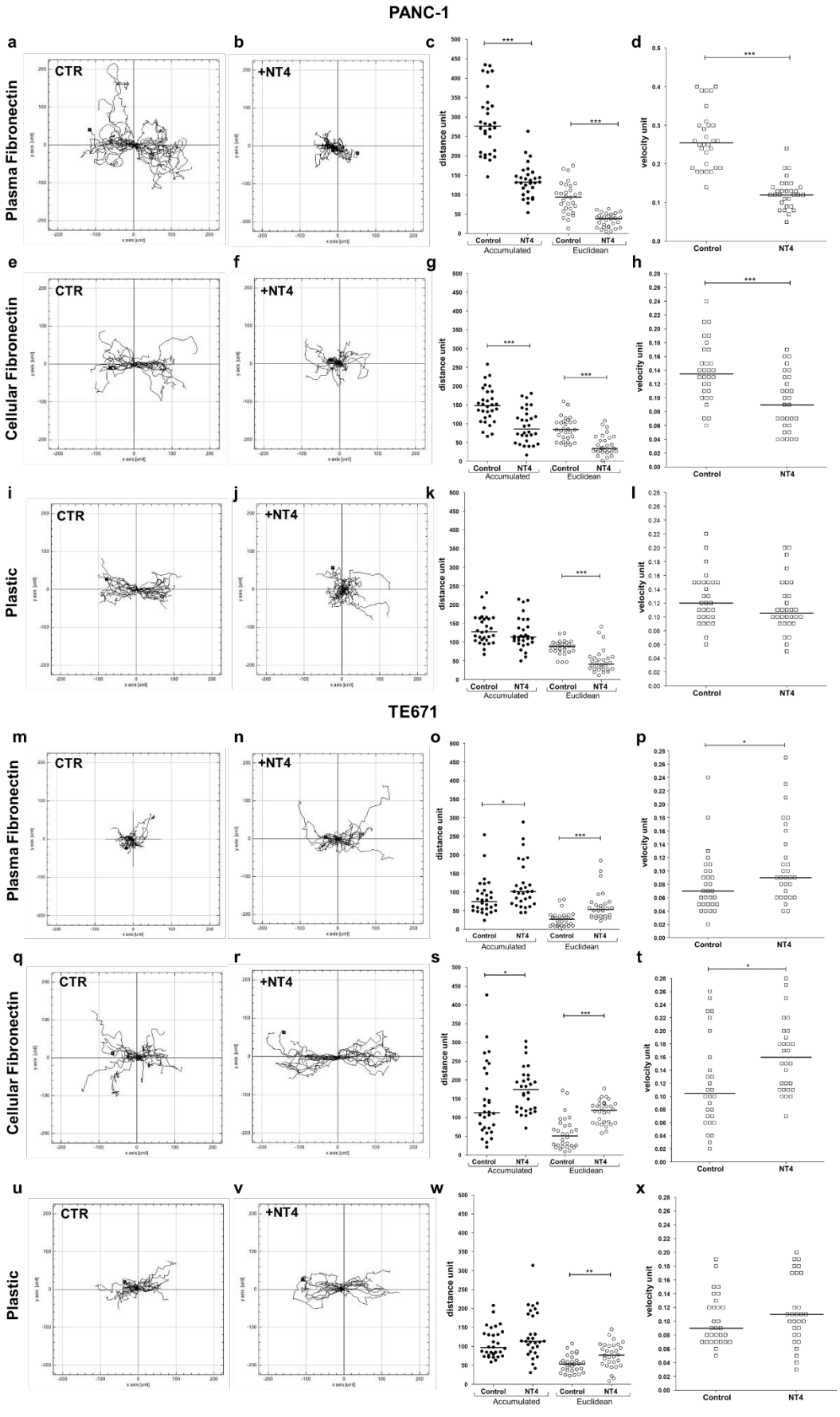
PANC-1
a
b
c
d
Plasma Fibronectin
CTR
+NT4
distance unit
velocity unit
Control
NT4
Accumulated
Euclidean
e
f
g
h
Cellular Fibronectin
i
j
k
l
Plastic
TE671
m
n
o
p
q
r
s
t
u
v
w
x

Fig. 3 Directionality and velocity of PANC-1 (a-l) and TE671 (m-x) cancer cell migration analyzed by time lapse microscopy. Cancer cells, cultured on plasma fibronectin, cellular fibronectin or uncoated plastic wells were incubated with (+ NT4) and without (CTR) 10 μM NT4. Cells were imaged every 10 min for 18 hours post-wounding and their paths were plotted on a polar grid. Each plot represents 30 individual cell tracks. The accumulated distance (filled circle), Euclidean distance (empty circle) and velocity (empty square) of each cell track are reported in the box plot graph. Median value is indicated by the black line. * $p < 0.05$, ** $p < 0.01$, *** $p < 0.001$ calculated using one-tailed Student t-test; $n = 30$.

The accumulated distance gives information on cell velocity, while Euclidean distance reflects the orientation of cell migration.

As shown in Fig. 3, accumulated distance and velocity of untreated PANC-1 cells were higher on plasma fibronectin (Fig. 3c,d) than on cellular fibronectin (Fig. 3g,h) ($p<0.0001$ for both accumulated distance and velocity) or on uncoated plastic wells (Fig. 3k,l) ($p<0.0001$ for both accumulated distance and velocity). Treatment of PANC-1 with NT4 peptide produced a significant decrease in cell velocity and in both accumulated and Euclidean distance on plasma and cellular fibronectin, whereas for cell migrating on plastic, the inhibition of cell migration produced by NT4 seems to be ascribed to an inhibition on cell orientation rather than velocity. In facts, differences of both accumulated distance and velocity between controls and cells treated with NT4 are not statistically significant for cells migrating on plastic, while differences in Euclidean distance are significant. (Fig. 3a-l).

The accumulated distance and velocity of migrating untreated TE671 cells were significantly lower than those of untreated PANC-1 cells on plasma fibronectin and uncoated wells ($p<0.0001$ on plasma fibronectin and $p<0.05$ on plastic, for both accumulated distance and velocity), whereas untreated TE671 cells seemed to have higher velocity and more directional trajectories when plated on cellular fibronectin than on plasma fibronectin ($p<0.01$ for both accumulated distance and velocity; $p<0.001$ for Euclidean distance. Moreover, untreated TE671 cells covered a smaller Euclidean distance, compared to untreated PANC-1 cells on all supports, which means they moved on trajectories with

poor orientation ($p<0.0001$ for plasma fibronectin and plastic; $p<0.01$ for cellular fibronectin). In the presence of NT4, TE671 cells not only migrated with larger accumulated distances, but also with more directional trajectories than control cells on all supports. Treatment of TE671 cells with NT4 produced an increase in cell velocity and both accumulated and Euclidean distance on either plasma or cellular fibronectin. On uncoated wells, as for PANC-1 cells, the effect of NT4 was only significant as increased Euclidean distance.

The results of analysis of single cell tracks reinforced our previous findings on the inhibitory effect of the sulfated GAG-specific peptide on directional migration of PANC-1 cells and suggested that sulfated GAG chains are involved differently in migration of TE671 with respect to PANC-1 cells. Sulfated GAGs appear to be involved in the regulation of oriented migration on all sorts of coating, whereas regulation of cell velocity by sulfated GAGs seems to be dependent on ECM proteins.

In order to test whether different migration phenotypes in these two-dimensional wound healing experiments corresponded to different cell invasiveness *in vitro*, and to analyze the effect of HSPG binding by NT4 peptide on *in vitro* invasiveness of different cancer cells, we tested migration of the three cancer cell lines in transwell invasion assays.

The transwell invasion assays is considered a reliable *in vitro* assay for cell invasiveness and completely confirmed the 2D migration results in the three cancer cell lines. PANC-1 cell migrated efficiently through the collagen coated membrane and migration was inhibited by NT4, whereas untreated TE671 were much less effective in migrating through the membrane than untreated PANC-1 cells and migration was clearly stimulated by the sulfated GAG-specific peptide. HT29 were not capable of migrating through the membrane and this was not modified by the NT4 peptide (Fig. 2d,e).

Different expression of syndecans and glypicans in PANC-1, TE671 and HT29 cancer cell lines

Since NT4 specifically recognizes sulfated GAGs and cancer cells can express different HSPGs with similar sulfated GAG chains, we analyzed expression of syndecan and glypican core proteins in the three cancer cell lines where analogous binding of NT4 produced very different effects in cell

adhesion, migration and invasiveness. Expression of syndecans and glypicans in PANC-1, TE671 and HT29 cancer cell lines was analyzed by qRT-PCR. We found generally lower expression of glypicans than syndecans. TE671 cells showed high expression of syndecan 2 and syndecan 3, both scarcely expressed by PANC-1 and HT29 cells, which conversely expressed syndecan 4 more than did TE671 cells. Syndecan 1 was scarcely expressed by all cell lines with the exception of HT29 (Fig. 4a).

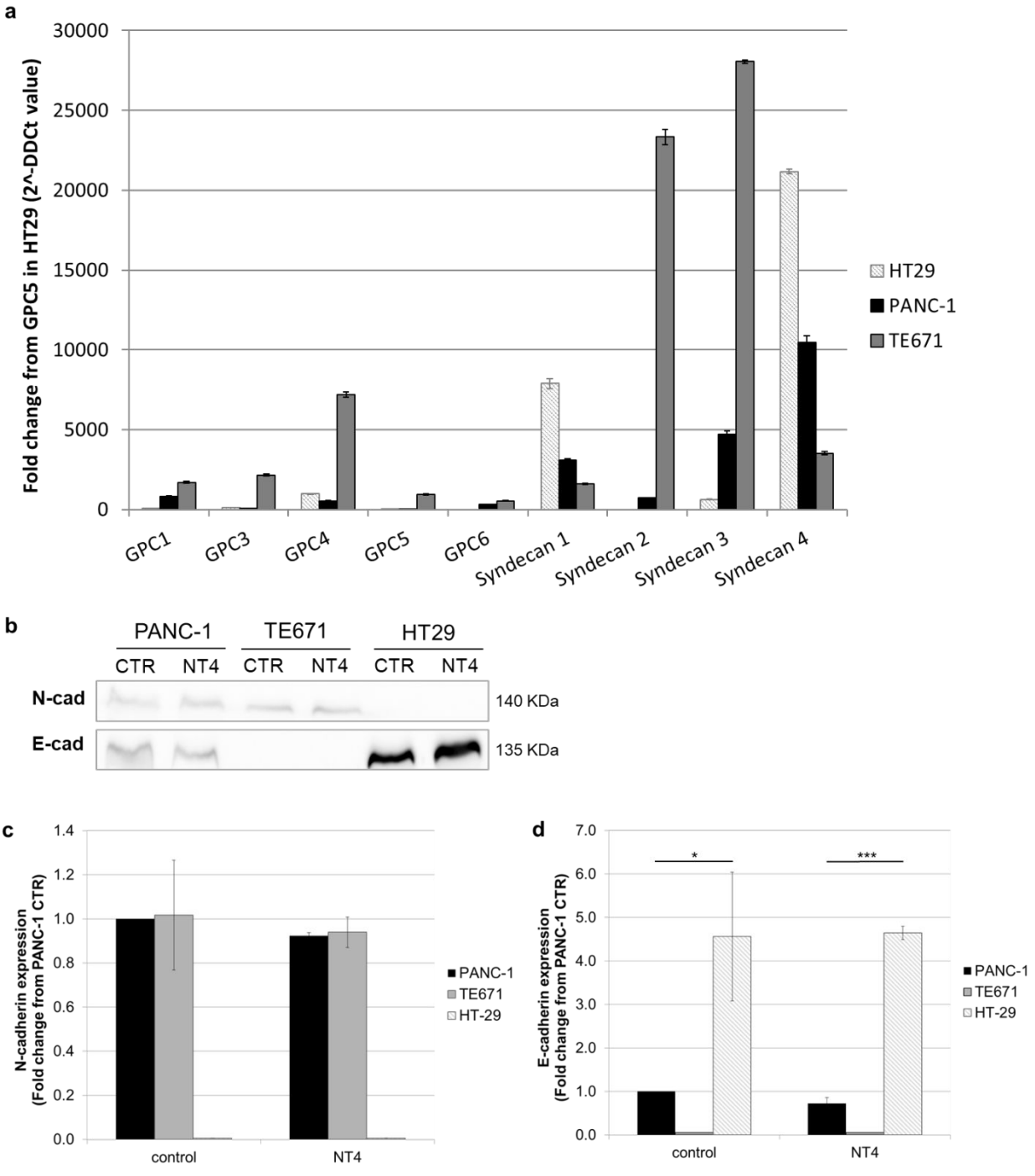

Fig. 4 a) Quantitative real-time PCR analysis of expression of human glypicans and syndecans in PANC-1, TE671 and HT29 cell lines. Gene expression data was normalized against β-actin and expressed as fold change with respect to glypican 5 in HT29 (the least expressed HSPG) ± SD. b-d) Western blot of N- and E-cadherin expression in PANC-1, TE671 and HT29 cells treated with 10 μM of NT4. Densitometry analysis, carried out using ImageJ software, was normalized to PANC-1 control. Errors bars represent SD. *$p < 0.05$ and *** $p<0.001$ by one-tailed Student t-test.

Different expression of E and N-cadherin in PANC-1, TE671 and HT29 cancer cell lines

E- and N-cadherins are considered hallmarks of cancer cell epithelial and mesenchymal phenotype, which correspond to different cell-cell and cell-ECM adhesions, consequently resulting in different cell migration propensity. Considering the different migration behavior of the three selected cell lines and the very different effect produced by NT4 peptide on both adhesion and migration of the same cell lines, we analyzed the expression of E-cadherin and N-cadherin in PANC-1, TE671 and HT29 cells by western blotting (Fig. 4b). Cadherin profile is different in the three cell lines, with PANC-1 cells expressing both E- and N- cadherin, TE671 expressing N-cadherin and not E-cadherin and HT29 expressing E-cadherin and not N-cadherin. Expression of both E- and N-cadherin was not affected by incubation of cells with NT4 peptide in all three cell lines (Fig. 4c,d).

Inhibition of cell directional migration by NT4 is accompanied by disruption of actin organization and increased filopodia

Binding of the sulfated GAG-specific peptide to different cancer cells resulted in either inhibition or enhancement of both directional migration and invasiveness in PANC-1 and TE671 cells, respectively. These cell lines express different cadherins and syndecans, which may be associated with different signaling pathways that regulate cytoskeletal rearrangement and cell migration.

NT4-induced modification of actin filament organization was tested in PANC-1 and TE671, either on cells plated at sub-confluent concentration, which do not receive stimuli for directional migration

(here indicated as static condition) or on migrating cells, in wound-healing experiments. We extended the analysis to HT29 cells, which bind NT4, and where NT4 can efficiently inhibit adhesion to different substrates but which are not capable of 2D or transwell migration.

Confocal microscopy of PANC-1 cells plated on cellular fibronectin and analyzed in static and migrating conditions (Fig. 5a,b) clearly showed that under both conditions NT4 produced disorganization of cancer cell actin filaments and stress fibers, simultaneously inducing an increase in filopodia, which gives the cells a typical "sea urchin" appearance.

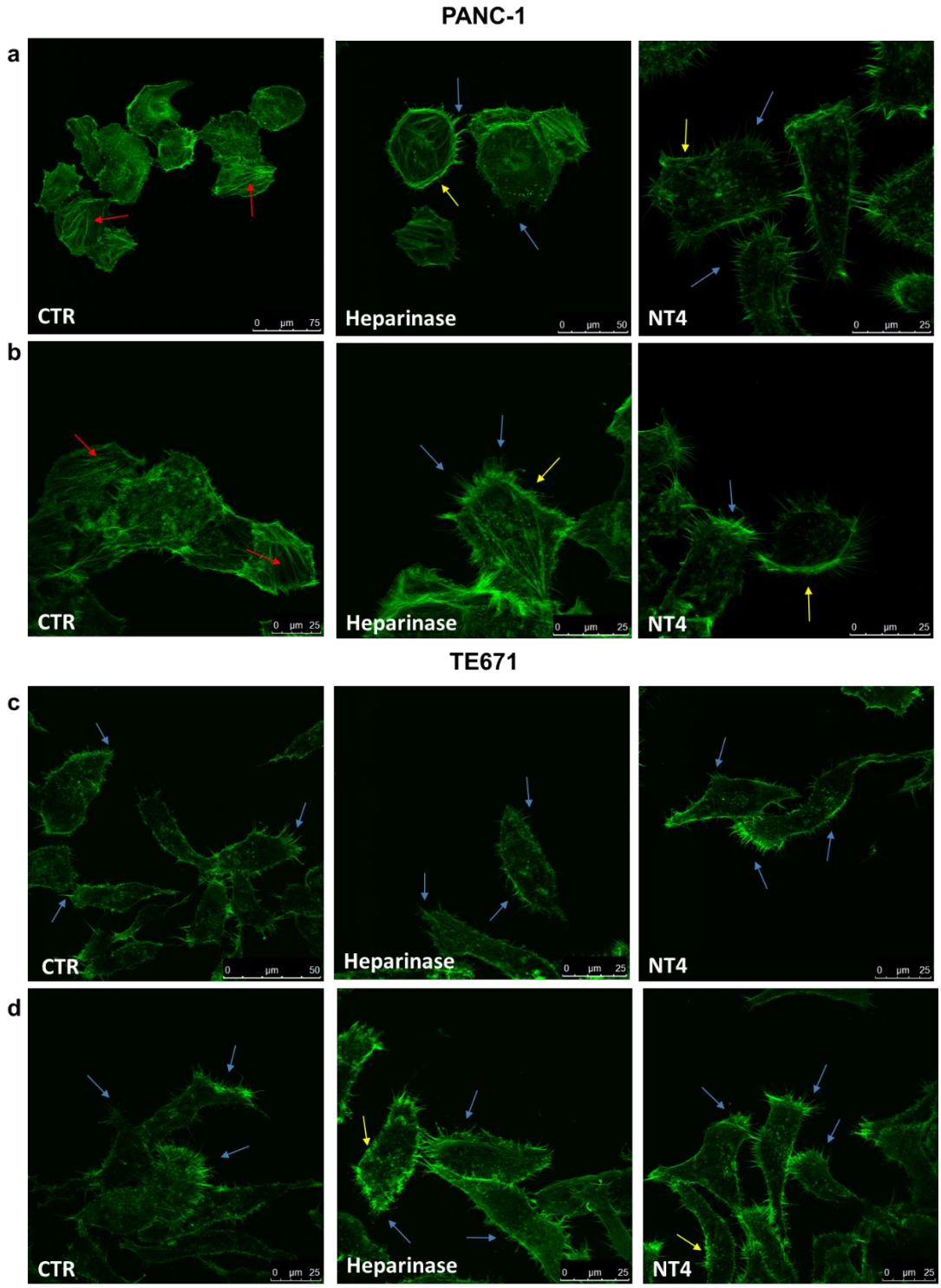

Fig. 5 Effect of NT4 peptide and heparinase on actin organization in PANC-1 and TE671 cells. Confocal microscope analysis of actin organization using phalloidin-Alexa Fluor 488 on PANC-1 cells under static (a) and migrating (b) conditions and TE671 cells under static (c) and migrating (d) conditions, plated on fibronectin-coated wells. Each series of images shows cells under no treatment (CTR), treatment with 0.03 IU/ml heparinase I/III blend or treatment with 10 μM NT4. Red arrows

indicate stress fibers, blue arrows indicate filopodia and yellow arrows indicate actin filaments accumulating under cell membranes.

In PANC-1 cells treated with NT4, actin filaments accumulated under cell membranes and in filopodia, while directionally organized stress fibers were lost. A similar although generally less pronounced effect was produced in the same cells by heparinase treatment. The spiky cell morphology caused by NT4 in PANC-1 cells has already been reported in cancer and normal cells migrating on 2D substrates under different experimental conditions. In different cases, disassembly of actin filament organization was accompanied by an increase in cell filopodia. This was obtained by treating cells with heparinase,[27,28] by silencing syndecan 4[27,29] or by interfering with cell signaling that controls the coordination of actin filament assembly, such as by silencing or mutating components of actin nucleators[30,31] or by silencing GTPases of the RHO family, particularly Rac1.[32,33]

Immunofluorescence staining of actin filaments in TE671 cells showed that their organization was very different from that of PANC-1 cells (Fig. 5c,d). Untreated TE671 cells showed many more filopodia than untreated PANC-1 cells, both under static conditions and during migration in wound healing experiments (Fig. 5c,d). Moreover, directionally organized stress fibers were scarce even in migrating TE671. The general organization of filopodia and actin filament in untreated TE671 cells, whether under static or migrating conditions, was very similar to that of PANC-1 cells after treatment with NT4. Interestingly and unlike what we observed in PANC-1 cells, treatment of TE671 with heparinase or NT4 did not significantly modify cell morphology or actin filament organization.

HT29 cells, which are unable to migrate, have round morphology without projections, very different from PANC-1 and TE671 cells. When analyzed at sub-confluence conditions, HT29 cells showed dispersed actin filaments, not organized into directional fibers, and this condition was not modified by treatment with NT4 (Fig. supplementary S2). Even if not migrating, when HT29 cells were analyzed in wound-healing experiments, they showed stress fibers and actin clustered under the cell

membrane (Fig. supplementary S2), which were less evident at sub-confluence (static condition). Not even this condition was modified by NT4.

Distibution of cadherins in migrating PANC-1, TE671 and HT29 cells

Considering the different migration phenotype of PANC-1, TE671 and HT29 cells and their diverse cadherin profiles, the possible effect produced by NT4 on the distribution of E- and N-cadherin in the three cell lines was analyzed by confocal microscopy in wound-healing experiments.

In untreated PANC-1 cells E-cadherin and N-cadherin showed similar distribution, though E-cadherin was more evident than N-cadherin, in agreement with results from protein expression. Both E- and N-cadherin were clearly evident at contacts among cells, and were less expressed in cells on the migration front. Both E- and N-cadherin were scarcely evident where actin was organized in projections and completely disappeared in migrating isolated cells. Despite the disorganization of actin fibers and the increased filopodia, produced by the anti-sulfated GAG peptide, the organization of both E- and N-cadherin did not appear to be modified by treatment with NT4 (Fig. 6).

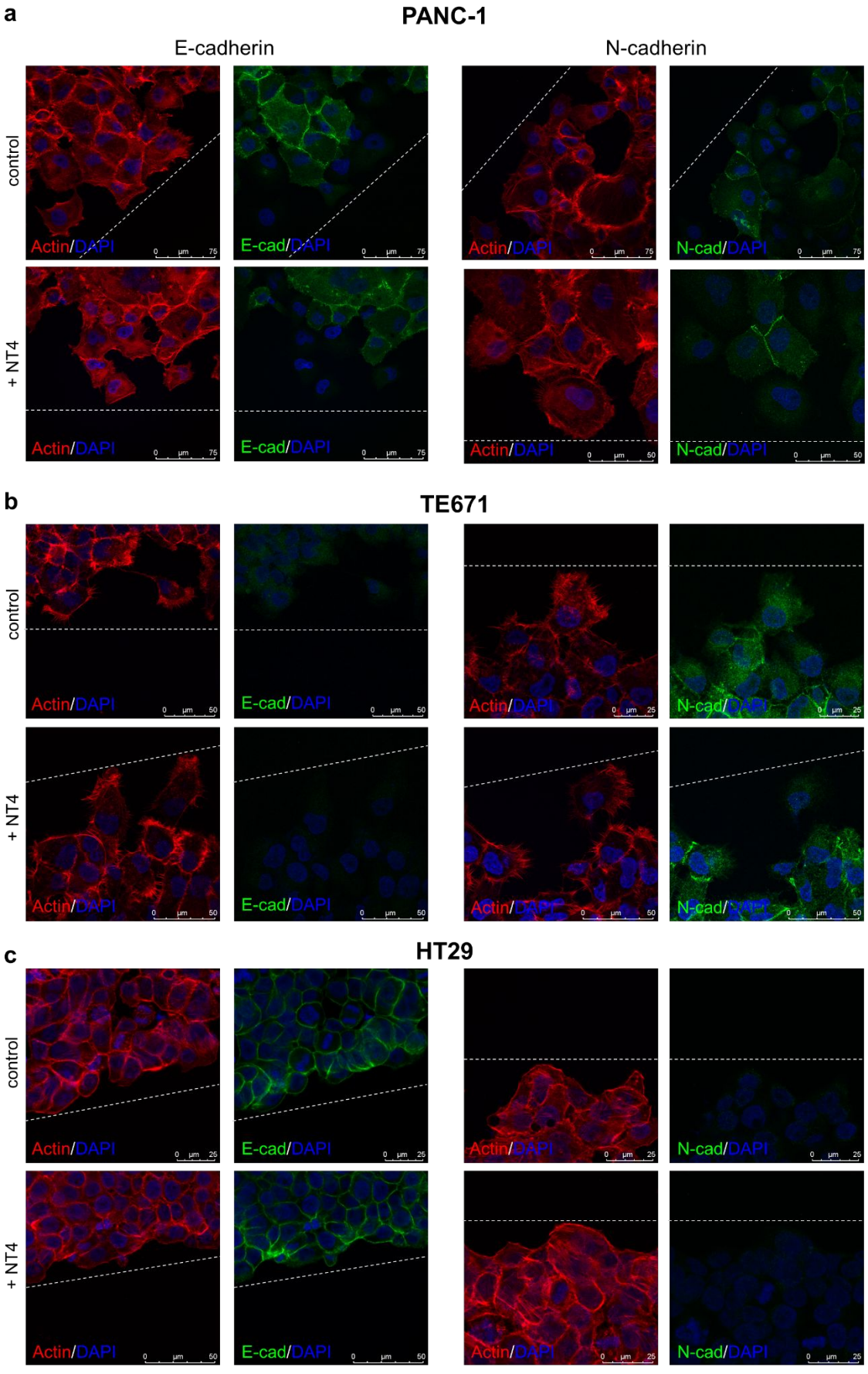

Fig. 6 Effect of NT4 peptide on N- and E-cadherin distribution in PANC-1, TE671 and HT29 cells.

Confocal microscope analysis of N- and E-cadherin (green signal) and actin (red signal) in PANC-1 (a), TE671 (b) and HT29 (c) cells under migrating conditions. Each series of images shows cells under no treatment (control) or treatment with 10 μM NT4 (+NT4). Nuclei are stained with DAPI (blue signal). The dotted lines indicate the cell migration front.

TE671 untreated cells do not express E-cadherin, which was in fact not detected, while N-cadherin was clearly evident at cell-cell contacts and similarly to PANC-1 cells, it was less expressed in cells on the migration front and was not evident in isolated migrating cells. Again, NT4 did not modify N-cadherin distribution in TE671.

HT29 cells express E-cadherin and not N-cadherin. HT29 cells are unable to migrate and E-cadherin was clearly evident at cell-cell contacts and all around the cell membrane, even on the migration front. Treatment with NT4 did not modify E-cadherin distribution.

NT4 does not modify β1 integrins or FAK activation

Since NT4 binding to sulfated GAG chains has very different effects on adhesion and migration of different cancer cells, as well as on actin cytoskeletal organization and cell morphology, and since β1 integrins and related focal adhesion kinase (FAK) are considered crucial for promoting actin filament organization and directional migration of cells,[34] we tested the effect of NT4 peptide on β1 integrins and FAK activation in the same three cancer cell lines. PANC-1 and TE671 cancer cells were incubated with NT4 under static conditions and during migration in wound healing experiments. Total and activated β1 integrins were stained with specific antibodies. No difference in distribution of total or activated β1 integrins was detected in PANC-1 or TE671 cells by confocal microscopy (Fig.7a-d). The amount and distribution of total and activated β1 integrins was also analyzed in HT29 under static conditions and in wound healing experiments. Even in HT29, no modification was detected in immunofluorescence on treatment with NT4 (Fig. 7e,f).

This result was confirmed by flow cytometry. In the three cell lines, recognition of β1integrins and activated β1integrins by the respective antibodies was not affected by preliminary incubation with NT4 (Fig. 7g,i). In line with this result, we also found that NT4 did not modify the amount of total FAK or activated phospho-FAK (pFAK Tyr397) in PANC-1 or TE671 (Fig. 7j,k). In HT29 cells, FAK and pFAK were not significantly modified by NT4, but the expression of pFAK was clearly higher than in PANC-1 and TE671 (Fig. 7j,k).

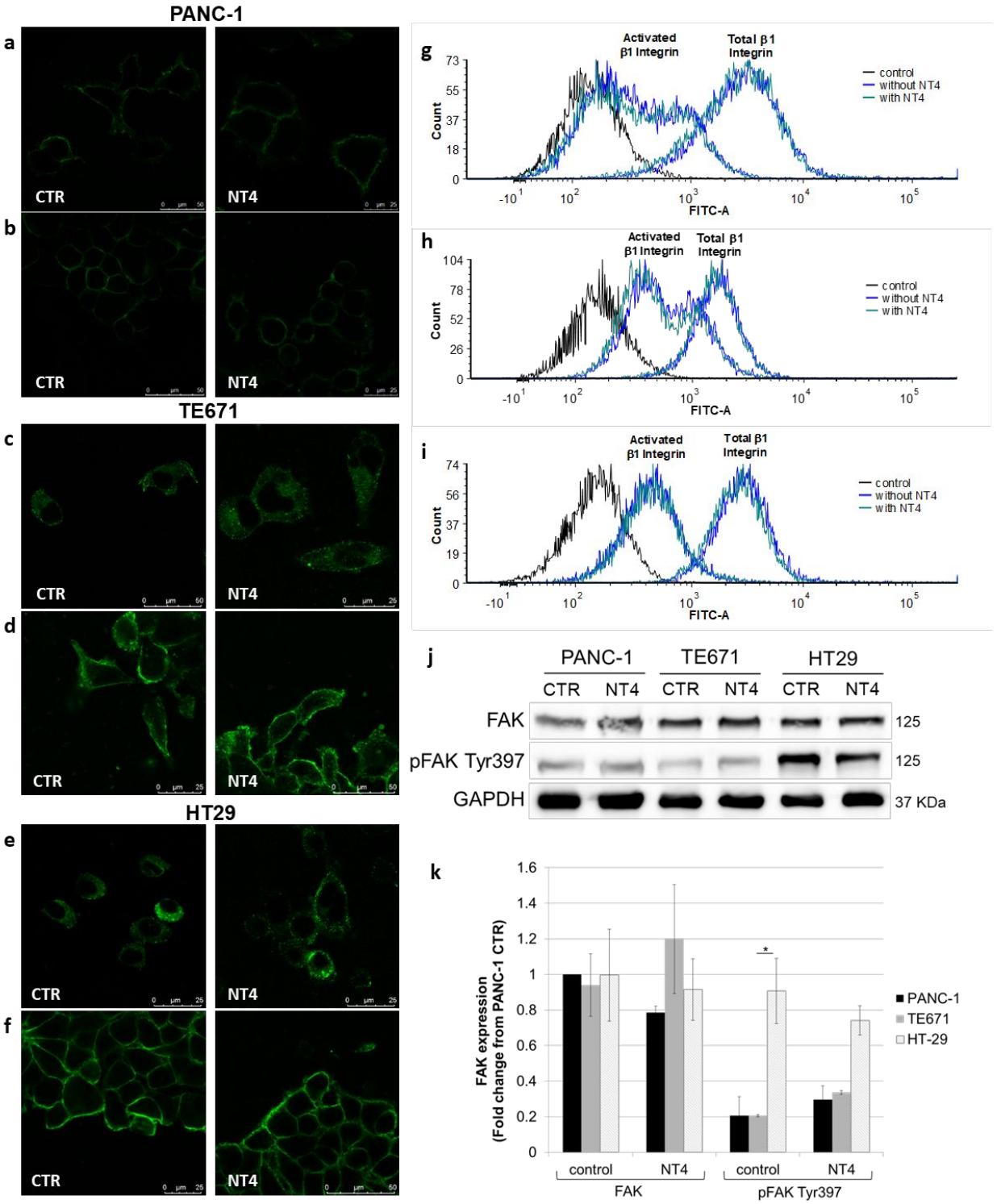
PANC-1
a
CTR
NT4
b
CTR
NT4
TE671
c
CTR
NT4
d
CTR
NT4
HT29
e
CTR
NT4
f
CTR
NT4
g
Activated β1 Integrin
Total β1 Integrin
control
without NT4
with NT4
Count
FITC-A
h
Activated β1 Integrin
Total β1 Integrin
control
without NT4
with NT4
Count
FITC-A
i
Activated β1 Integrin
Total β1 Integrin
control
without NT4
with NT4
Count
FITC-A
j
PANC-1
TE671
HT29
CTR
NT4
FAK
pFAK Tyr397
GAPDH
125
125
37 KDa
k
FAK expression
(Fold change from PANC-1 CTR)
PANC-1
TE671
HT-29
control
NT4
FAK
pFAK Tyr397

Fig. 7. Effect of NT4 peptide on activation β1 integrins and FAK in PANC-1, TE671 and HT29 cells. Confocal microscopy analysis of anti-activated β1 integrin monoclonal antibody binding to PANC-1 cells under static (a) and migrating (b) conditions, TE671 cells under static (c) and migrating (d) conditions and HT29 cells under static (e) and migrating (f) conditions, plated on fibronectin-coated wells. Each series of images shows cells under no treatment (CTR) or treatment with 10 μM NT4. Analogous experiments were done for detecting total β1 integrins, obtaining completely comparable results (not shown). Flow cytometry analysis of anti-activated β1 integrin monoclonal antibody and anti-total β1 integrin antibody binding to PANC-1 (g), TE671 (h) and HT29 (i) cells with or without 10 μM NT4. Western blot of FAK and pFAK in the three cell lines (j, k). Densitometry analysis, carried out using ImageJ software, was normalized to PANC-1 control. Errors bars represent SD. *$p < 0.05$, ** $p<0.01$ and *** $p<0.001$ by one-tailed Student t-test.

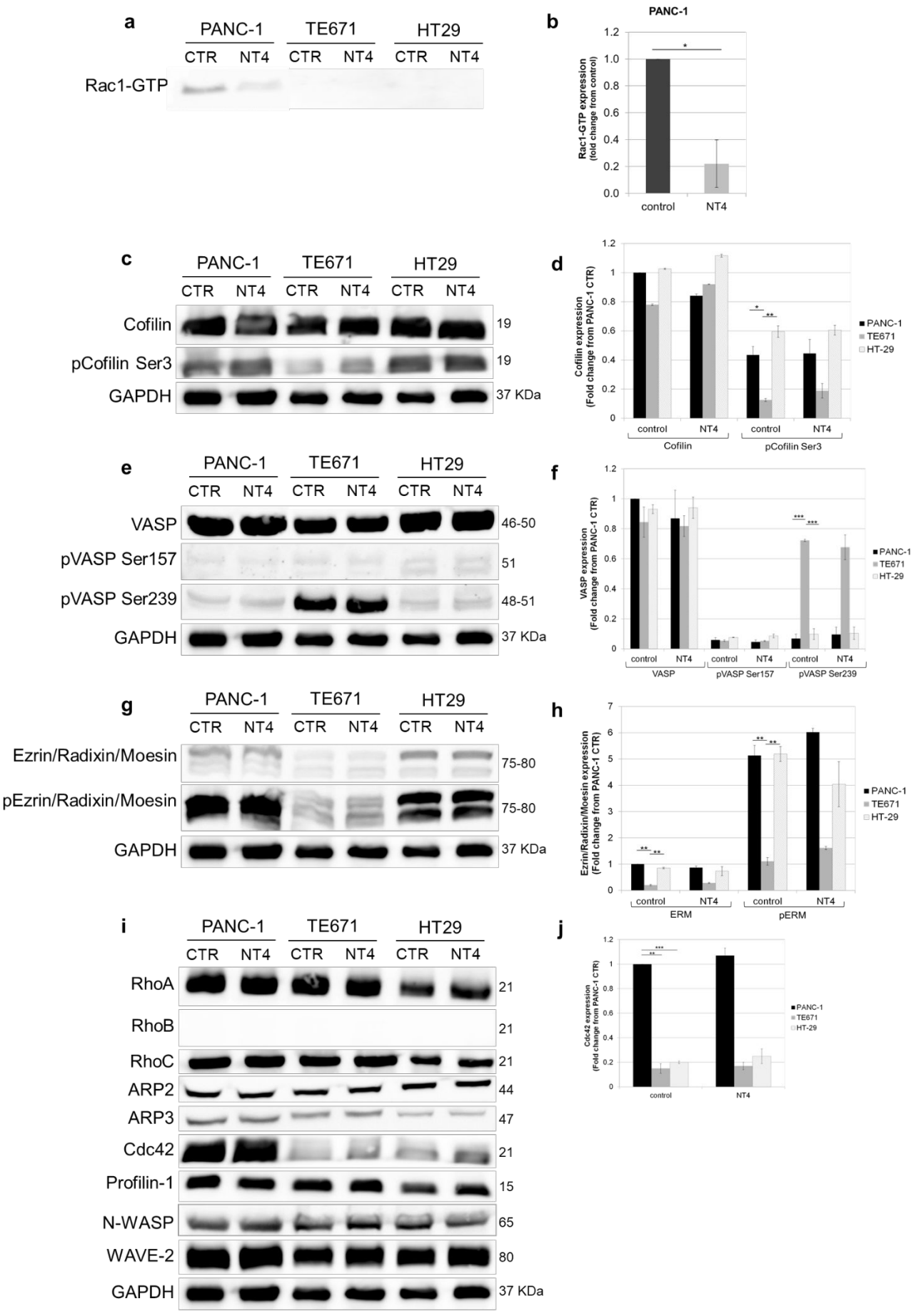
a
PANC-1
TE671
HT29
CTR
NT4
Rac1-GTP
b
PANC-1
Rac1-GTP expression (fold change from control)
control
NT4
c
Cofilin
pCofilin Ser3
GAPDH
19
37 KDa
d
Cofilin expression (Fold change from PANC-1 CTR)
pCofilin Ser3
PANC-1
TE671
HT-29
e
VASP
pVASP Ser157
pVASP Ser239
46-50
51
48-51
f
VASP expression (Fold change from PANC-1 CTR)
pVASP Ser157
pVASP Ser239
g
Ezrin/Radixin/Moesin
pEzrin/Radixin/Moesin
75-80
h
Ezrin/Radixin/Moesin expression (Fold change from PANC-1 CTR)
ERM
pERM
i
RhoA
RhoB
RhoC
ARP2
ARP3
Cdc42
Profilin-1
N-WASP
WAVE-2
21
44
47
15
65
80
j
Cdc42 expression (Fold change from PANC-1 CTR)

Fig. 8 Effect of NT4 on actin reorganization signaling in cancer cells with different migration phenotype. Western blot of Rac1-GTP (a-b), cofilin (c-d), VASP (e-f), Ezrin/Radixin/Moesin (g-h), RhoA, RhoB, RhoC, Apr2, Arp3, Cdc42, Profilin-1, N-WASP and WAVE-2 (i-j), in PANC-1, TE671 and HT29 cells treated with 10 μM NT4. GAPDH was used as endogenous control. Densitometry analysis, carried out using ImageJ software, was normalized to PANC-1 control. Values are reported as fold change with respect to PANC-1 control ± SD from three independent experiments. *$p < 0.05$, ** $p<0.01$ and *** $p<0.001$ by one-tailed Student t-test.

Actin reorganization signaling in PANC-1, TE671 and HT29 cancer cell lines

Expression of proteins involved in actin reorganization and cell protrusions dynamics was compared in the three cell lines, together with possible modifications induced by incubation with the sulfated GAG-specific NT4 peptide.

Expression of proteins involved in cell migration endocellular signaling were different in untreated TE671, PANC-1 and HT29 cells. In particular, activated Rac1-GTP was not detectable in untreated TE671 and HT29 cells, but was evident in untreated PANC-1 cells, where it was also clearly decreased after treatment with NT4 (Fig. 8a,b).

Interesting data came from analysis of expression of different proteins involved in actin reorganization, nucleation and assembly in the same three cell lines.

Cofilin is an important regulator of actin dynamics, which acts by severing F-actin, thus creating free barbed ends for possible actin polymerization and also promoting disassembly of the branched actin network,[35] by counteracting the action of the Arp2/3 complex, which is known to mediate actin filament branching leading to lamellipodia, downstream Rac1 and WAVE complex activation.[36,37] Phosphorylated cofilin (p-cofilin) is inactive[38] and there are indications that inactivation of cofilin promotes lamellipodia-driven directional migration,[39] whereas constitutively active non phosphorylated cofilin is associated with increased filopodia.[40] Our results are in agreement with previous indications of cofilin activity. Indeed, lamellipodia-driven directional migration was much higher in PANC-1 cells, which have higher levels of inactive p-cofilin than TE671 cells (Fig. 8c,d),

which in fact have fewer lamellipodia, more filopodia and lower expression of p-cofilin with respect to total cofilin, than PANC-1 cells (Fig. 5 and 8).

VASP is a member of the Ena/VASP family of actin-binding and anti-capping proteins that promote actin filament elongation, particularly when these are assembled in linear bundles, such as in filopodia.[41] The molecular mechanisms of VASP activity, including its regulation by kinases[42] and downstream effects, are still elusive.[43] VASP has an anti-branching effect that counteracts the activity of the Arp2/3 complex. Its anti-branching activity may explain VASP's effect on filopodia, rather than on lamellipodia elongation. VASP may be phosphorylated at Ser157 and Ser239, which may have opposite effects on actin filament organization, wherein pSer157 seems to promote and pSer239 to suppress actin assembly, negatively affecting focal adhesion and lamellipodia.[44,45] The total expression of VASP was comparable in the three cell lines, whereas TE671 cells had much higher expression of pVASP Ser239, which was not modified by treatment with NT4. pVASP Ser157 was nearly undetectable in all three cell lines (Fig. 8e,f).

Ezrin/Radixin/Moesin (ERM) proteins are essential for linking the actin cytoskeleton to the plasma membrane, where they can be recruited and concomitantly activated through phosphorylation at conserved threonine residues. The ERM proteins are crucial for organization of the apical domain of polarized epithelial cells and a lack of these proteins determines loss of polar organization and orientation.[46] Expression of ERM proteins, particularly in their phosphorylated form, was lower in TE671 than in PANC-1 and HT29 (Fig. 8g,h). The lower expression of ERM and pERM by TE671 may correlate with the chaotic migration observed in TE671 and also with previous findings on the importance of ERM in cell orientation.

RhoA and C were indifferently expressed by the three cell lines and no effect was observed upon treatment with NT4. The same can be said for Arp2/3, profilin-1, N-WASP and WAVE-2 (Fig. 8i). RhoB was not expressed by any cell line.

Another significant difference was detected in the expression of Cdc42, which was expressed less in TE671 and HT29 cells than in PANC-1 (Fig. 8i,j). Cdc42 is a Rho GTPase, analogue of Rac1, which

regulates actin polymerization by Arp2/3 mainly through activation of the WASP complex, instead of the WAVE complex, which is mainly activated by Rac1.[47] Defective expression of Cdc42 may account for misregulation of cell migration, which may be more dramatic when associated with defective activation of Rac1.

None of these differently expressed proteins were significantly modified by incubation of the three cell lines with NT4, with the notable exception of activated Rac1 in PANC-1 cells.

Discussion and Conclusions

Taking advantage of a tumor-targeting peptide tool that specifically recognizes sulfated GAGs, we analyzed the role of membrane HSPGs in adhesion and migration of cancer cell lines. Starting from a clearly different effect produced by the peptide on adhesion and migration of different cancer cells on solid supports, we identified different cell migration phenotypes and tested the possible role of HSPGs in each phenotype.

We found that cells migrating by steady and polarized lamellipodia, like PANC-1 cells, express syndecan 4 and both E- and N-cadherin. PANC-1 showed directional migration and invasiveness in trans-well experiments, which were both dramatically inhibited by blocking or removal of sulfated GAGs. Blocking of sulfated GAGs in these cells produced a switch to unsteady lamellipodia and increased filopodia, accompanied by inhibition of GTP-bound activated Rac1, with no concomitant effect on E- and N-cadherin distribution or on activation of either β1 integrins or FAK. Our results with PANC-1 cells seem to confirm the already reported possible involvement of syndecan 4 in lamellipodia-driven directional cell migration, which is associated with increased Rac1 activity.[29] This pathway may essentially be initiated in PANC-1 cells by adhesion of sulfated GAGs to ECM, since blocking the sulfated GAGs by NT4 inhibited cell adhesion to ECM proteins and also inactivated the Rac1 pathway, producing the cell modifications already reported to be associated with silencing of syndecan 4, or to Rac1 or Arp2/3 inactivation.[27,29-33] The high expression of inactive p-

cofilin and low expression of pVASP are in line with this model of PANC-1 lamellipodia-driven directional migration.

On the other hand, TE671 cells express N-cadherin and not E-cadherin and much more syndecan 2 than PANC-1 cells, they had no detectable basal Rac1-GTP, more pVASP Ser239, lower inactive p-cofilin and lower ERM than PANC-1 and HT29, and their migration was less directional, with unsteady lamellipodia and more abundant filopodia, compared to PANC-1 cells. In the case of TE671, the effect produced by the sulfated GAG-specific peptide was intriguing, since it had very little effect on cell adhesion to ECM proteins and induced an increase in cell migration, mostly caused by an increase in cell directionality, still with no modification in N-cadherin distribution or β1 integrins and FAK activation. Given the reported association of syndecan 2 with VASP activation,[48] and the known strong increase in VASP activity induced by its clustering,[49,50] we can speculate that by binding to sulfated GAG chains associated with syndecan 2, the tetra-branched NT4 peptide might increase its signaling, possibly by increasing VASP clustering, by means of multimeric binding.

Interesting data came from analysis of HT29 cancer cells. These cells were recognized by the sulfated GAG-specific peptide, which inhibited their adhesion to different supports. Nonetheless, HT29 were unable to migrate in wound healing and transwell experiments and treatment with peptide NT4 did not modify this condition. Like PANC-1 cells, HT29 expressed syndecan 4, but like TE671, HT29 lacked activated Rac1-GTP and showed lower expression of Cdc42, compared to PANC-1 cells (Fig. 8a,b,i,j). The ratio of total versus phosphorylated cofilin (Fig. 8c,d) and VASP (Fig. 8e,f) of HT29 was similar to that of PANC-1, whereas phospho-FAK was clearly higher than in PANC-1 and TE671 cells (Fig. 7j,k). Notably, differently from both PANC-1 and TE671 cells, HT29 cells have a typical epithelial phenotype with extensive cell-cell contacts and massive E-cadherin expression, which were maintained even in cells on the migrating front in wound healing experiments.

The cadherin phenotype and distribution in wound healing experiments, together with the expression of the main regulators of actin reorganization in HT29, compared to PANC-1 and TE671 cells suggest that down regulation of both E- and N-cadherin in cell-cell contacts, which appeared essential for 2D

migration of both PANC-1 and TE671 cells, is not dependent on HSPGs and precedes their engagement, which may instead be essential for guiding cell directionality in migrating cells. HT29 cells inability to migrate may then be associated to the absence of E-cadherin down regulation, prodromal to HSPG regulation of cell migration.

Our results suggest two different models of cancer cell migration: one is fast, directional, lamellipodia-driven and highly invasive; the other is slower, scarcely directional, filopodia-driven and less invasive. They correspond to two alternative endocellular signaling modes for actin filament assembly and organization. In these models, sulfated GAG chains may be associated to different signals in relation to the protein core of the HSPG they are linked to. In lamellipodia-driven directional migration, endocellular signaling may be activated by engagement of sulfated GAG chains of syndecan 4, and may work with –though not depend on– integrin-induced signaling to stabilize lamellipodia and keep cell migration on track by the Rac1-activated WAVE complex and subsequent Arp2/3-mediated actin nucleation and branching.

In cells displaying slower, scarcely directional migration, with few unsteady lamellipodia and high production of filopodia, endocellular signaling appears essentially independent of Rac1 with alternative involvement of VASP and cofilin. In filopodia-driven cell migration, increased directionality may be induced by syndecan 2 cross-linking, leading to increased VASP activation. In our experiments, this cross-linking may have been induced by multimeric binding of the sulfated GAG-specific tetra-branched peptide. In vivo, analogous cross-linking, leading to increased migration and invasiveness, may be induced by specific ligands, such as growth factors, morphogens or chemokines, binding to HSPGs. These models, where different HSPGs promote alternative signaling for cell migration, and where ligand binding to sulfated GAG chains carried by different syndecans can produce opposite effects on cancer cell behavior, may explain the many discordant results obtained on the possible pro- or anti-tumorigenic effects of HSPGs or their many ligands in different cancers or cancer cell lines. They should be carefully considered when designing anti-cancer drugs targeted at HSPGs or cell migration endocellular signaling.

Experimental Section

Materials

Dulbecco's modified Eagle's medium (DMEM) (ECB750IL), McCoy's 5A medium (BE12-688F), Penicillin/Streptomycin (ECB3001D) and fetal bovine serum (FCS) (ECS0180L) were from Euroclone (Pero, Mi, Italy); anti E- and N-cadherin antibodies (# 14472 and # 13116) actin nucleation and polymerization antibody sampler kit (#8606), actin reorganization antibody sampler kit (#9967), Rho-GTPase Antibody Sampler Kit (#9968), Active Rac1 Detection Kit (#8815), FAK antibody (#3285), Phospho-FAK Tyr397 Rabbit mAb (#8556), anti-rabbit IgG, HRP-linked Antibody (#7074), Blue Loading Buffer Pack (#7722) were purchased from Cell Signaling Technology (Danvers, MA, USA); anti-E-cadherin for immunofluorescence analysis (ab40772), anti β1 integrin monoclonal antibody (ab24693) were purchased from Abcam; anti activated β1 integrin monoclonal antibody (MAB2079Z) was from Millipore; Avidin-FITC (A2901), human collagen IV (C6745), fibronectin from human fibroblast (cellular fibronectin; F0556), fibronectin from human plasma (plasma fibronectin; F2006), PureCol collagen I (5074), heparinase I/III blend (H3917), Fluoroshield with DAPI (F6057), heparin sodium salt from porcine intestinal mucosa (H3149) and L-Glutamine (G7513) were purchased from Sigma Aldrich.

Anti-mouse IgG Alexa Fluor 488 (A11001), anti-rabbit IgG Alexa Fluor 546 (A11010), anti-GAPDH (AM4300) antibodies, Alexa Fluor 488 phalloidin (A12379) were purchased from Invitrogen; SuperSignal® Molecular Weight Protein Ladder (84785), anti-mouse IgG, HRP-linked Antibody (#31430) and Pierce™ 16% Formaldehyde (w/v) methanol-free (28908) were from Thermo Scientific; Nitrocellulose membranes and the reagents for enhanced chemiluminescence (ECL) detection were obtained from Amersham Life Science (Pittsburgh, USA).

Peptide synthesis

Peptide synthesis was performed with standard Fmoc chemistry as previously described.[24]

Purity of all compounds is > 95% as determined by HPLC. All compounds were also characterized on a BrukerUltraflex MALDI TOF/TOF Mass Spectrometer.

Cell lines

PANC-1 human pancreas adenocarcinoma, HT-29 human colon adenocarcinoma, MCF-7 and MDA-MB 231 human breast adenocarcinoma, T24 human bladder carcinoma, A375 human melanoma and TE671 human rhabdomyosarcoma were grown in their recommended media supplemented with 10% fetal bovine serum at 37°C, 5% CO_2. Cell lines were purchased from ATCC and cell profiling was analyzed to authenticate human cell lines (BMR Genomics).

Flow cytometry

All experiments were performed using 2 x10^5 cells in 96-well U-bottom plates. All dilutions were performed in PBS, containing 5 mM EDTA and 1% BSA.

NT4 binding

Cells were incubated with 500 nM biotinylated NT4 for 30 min at room temperature. Inhibition of NT4 binding by heparin was carried out incubating cells with 500 nM biotinylated NT4 and 20 μg/ml heparin. Cells were finally incubated with 1 μg/ml Streptavidin-FITC.

β1 integrins

Cells, previously treated with 10 μM NT4 for 3 h at 37°C, were harvested and incubated with 2.5 μg/well anti activated β1 integrin monoclonal antibody for 1 h at room temperature or incubated with 0.5 μg/well anti total β1 integrin monoclonal antibody for 30 min at room temperature. Cells were finally incubated for 30 min at room temperature with an anti-mouse IgG Alexa Fluor 488 antibody diluted 1:500. Ten thousand events were analyzed using a BD FACSCanto II (Becton Dickinson, NJ USA) or FACS Guava (Millipore). Results were analyzed by FCS Express 6 flow software.

Cancer cell adhesion assay

96-well cell culture plates were coated with 20 μg/ml human collagen IV or with 10 μg/ml cellular fibronectin or plasma fibronectin for 2 h at 37°C. 1 × 10^5 cells/well were plated for 30 minutes at 37°C with different concentrations of NT4 (from 1 μM to 10 μM), fixed with PBS - 4% PFA for 15

minutes at room temperature and stained with 0.1% crystal violet in 200 mM MES (2-(N-morpholino) ethanesulfonic acid) pH 6.0 for 1 h at room temperature. The cells were then solubilized with 10% acetic acid and the absorbance was measured at 595 nm using a microplate reader.

Wound healing

PANC-1 (2.8×10^4), TE671 (5.2×10^4) and HT29 cells (7.7×10^4) were seeded on each side of a culture insert for live cell analysis (Ibidi, Munich, Germany). Inserts were placed in wells of an uncoated or pre-coated 24-well plate (10 μg/ml cellular fibronectin or plasma fibronectin for 2 h at 37°C) and incubated at 37°C and 5% CO_2 to allow cells to grow to confluence. Afterwards, inserts were removed with sterile tweezers and the cells were treated with 10 μM NT4 peptide in complete medium. The cells were allowed to migrate in the incubator of a DMi8 (Leica Microsystems) microscope. The same instrument was used to take a picture at time zero and every 10 min for 18 h. The time lapse image stacks were analyzed using ImageJ and the plug-in Chemotaxis and Migration Tool. Individual cells were randomly selected and tracked throughout the 18 h time period**.**

Transwell cell migration

Standard transwell inserts for 24-well plates (transparent PET membrane, 8.0 μm pore size, Corning), equilibrated with serum-free tissue culture medium for 2 h at 37°C, were coated with chilled neutralized PureCol collagen I. $5x10^4$ PANC-1, TE671 and HT29 cells diluted in serum-free medium containing 10 μM NT4 were placed in the upper chambers and the lower chambers were filled with medium containing 10% serum. After 24 h incubation at 37°C in a humidified atmosphere with 5% CO_2, the non-invasive cells that remained on the upper side of the insert membranes were removed using cotton swabs. The cells that invaded the lower side of the insert membranes were fixed with 4% PFA in PBS and stained with Crystal Violet. The entire image of stained cells was observed with a SP8 confocal microscope (Leica Microsystem) and were analyzed by ImageJ to count cells.

Real-time PCR

Total RNA samples were extracted from different human cancer cells with Trizol (Invitrogen, Milan, Italy). For quantitative RT-PCR, RNA samples were retrotranscribed using the High Capacity cDNA

synthesis kit (Applied Biosystems, Monza, Italy) and amplified on an Abi Prism 7000 instrument (Applied Biosystems, Monza, Italy) using the Taqman Universal PCR Master Mix (Applied Biosystems) according to the manufacturer's instructions.

The following human Taqman gene expression assays were used: GPC1 (Hs00157805_m1), GPC3 (Hs00170471_ml), GPC4 (Hs00155059_m1), GPC5 (Hs00270114_m1), GPC6 (Hs00170677_ml), SDC1 (Hs00174579_m1), SDC2 (Hs00299807_m1), SDC3 (Hs00206320_m1), SDC4 (Hs00161617_m1) and β-actin (Hs99999903_m1). Fluorescent signals generated during PCR amplifications were monitored and analyzed with Abi Prism 7000 SDS software (Applied Biosystems).

In order to determine the efficiency of each Taqman gene expression assay, standard curves were generated by serial dilution of cDNA, and quantitative evaluations of target and housekeeping gene levels were obtained by measuring threshold cycle numbers (Ct). A relative quantitative analysis was performed, using the 2-ΔΔCt value, where ΔCt = Ct (target) – Ct (endogenous control) and ΔΔCt = ΔCt (sample) – ΔCt (calibrator). Beta actin was used as endogenous control and the sample with the lowest expression was used as calibrator (Glypican 5 in HT29).

Immunofluorescence

PANC-1, TE671 and HT29 cells were plated in 24-well plates with cover glass slides previously coated with 10 μg/ml cellular fibronectin. Cells were treated with 10 μM NT4 in DMEM or 0.03 IU/ml heparinase I/III blend in DMEM for 3 h at 37°C, fixed with PBS-4% PFA methanol free for 10 min, permeabilized with PBS-0.25% Triton X-100 for 15 min, saturated with PBS-5% bovine serum albumin (BSA) for 60 min and then incubated with Alexa Fluor 488 phalloidin 1:40 in PBS-1% BSA for 30 min.

For the analysis of activated β1 integrins, PANC-1, TE671 and HT29 cells were treated with NT4 as above, fixed with PBS-4% PFA for 10 min, saturated with PBS-5% BSA for 60 min and incubated with anti-activated β1 integrin monoclonal antibody 1:250 in PBS-1% BSA for 2 h at room

temperature. Cells were finally incubated for 30 min at room temperature with an anti-mouse IgG Alexa Fluor 488 antibody diluted 1:500.

For the analysis of E and N-cadherin, PANC-1, TE671 and HT29 cells were treated with NT4 as above, fixed with PBS-4% PFA for 10 min, saturated with PBS-5% BSA for 60 min and incubated with anti E-cadherin (1:500) and N-cadherin (1:200) antibodies in PBS-1% BSA for 2 h at room temperature. Cells were finally incubated for 2 h at room temperature with an anti-rabbit IgG Alexa Fluor 546 antibody diluted 1:1000. Samples, mounted using Fluoroshield with DAPI, were analyzed by confocal laser microscope (Leica TCS SP8) with 364-495 nm excitation and 458-518 nm emission filters for DAPI and Alexa Fluor 488, respectively. All images were processed using ImageJ software (NIH).

Western blot

Cells were seeded in six-well plates (1.5×10^6 cells per well), previously coated with 10 µg/ml plasma fibronectin and maintained overnight in a CO_2 incubator. Cells were treated with 10 µM NT4 in DMEM for 3 h at 37°C and lysed according to the antibody supplier's instructions (Cell Signaling). 20 µl/lane total proteins was separated by 12% SDS-PAGE and transferred to a nitrocellulose membrane. The membrane was blocked with 5% w/v BSA in TBS containing 0.1% Tween20 for 1 h at room temperature and then incubated overnight at 4°C with specific antibodies diluted 1:1000 in 5% w/v BSA or nonfat dry milk in TBS containing 0.1% Tween20, according to the antibody supplier's instructions. After washing with TBS containing 0.1% Tween20, the membrane was incubated for 1 h with horseradish peroxidase-conjugated anti-rabbit and anti-mouse IgG antibodies diluted 1:2000 in 5% w/v nonfat dry milk in TBS containing 0.1% Tween20. Signals were detected using Image LAS4010 (GE Healthcare).

Pulldown Assay

Rac1 activity was measured by pulldown assay using the active Rac1 detection kit according to the manufacturer's instructions. In brief, 500 µg of protein lysates were incubated with beads pre-coupled with GST–PAK1-PBD under rotation at 4°C for 60 min. The beads were washed and the proteins

bound to the beads were separated by SDS-PAGE. The amounts of active Rac1 were determined by immunoblotting analysis. Signals were detected using Image LAS4010 (GE Healthcare).

Statistical Analysis

All experiments were repeated at least three times and the data was presented as mean ± SD. The significance of differences was analyzed by one-tailed Student's t-test using GraphPad Prism 5.03 software; p values are reported in figure legends.

Supporting Information

Schematic representation of Euclidean and accumulated distance (Fig. S1); Effect of NT4 peptide on actin organization in HT29 cells (Fig. S2); Video of PANC-1, TE671 and HT29 cells migrating in wound healing assays, with or without 10 μM NT4 (Videos S1-6).

Molecular-string file.

Corresponding Author: Prof. Luisa Bracci, Department of Medical Biotechnologies, University of Siena, 53100 Siena. Phone: +39 0577 232020; Email: luisa.bracci@unisi.it; ORCID: 0000-0002-0738-5746

Author Contributions: # L.D. and J.B. contributed equally to the paper.

Notes: The authors declare no competing financial interest.

Acknowledgements

This work was supported by Italian Association for Cancer Research grant (AIRC IG 2014 Id. 15564) and by Istituto Toscano Tumori ITT grant 2013.

Abbreviation used

CS, chondroitin sulfate; CTR, control; E-cad, E-cadherin; ECM, extracellular matrix; ERM, Ezrin/Radixin/Moesin; FAK, focal adhesion kinase; GAG, glycosaminoglycan; GPC, glypican; HS, heparan sulfate; HSPG, Heparan sulfate proteoglycan; N-cad, N-cadherin.

References

1. Chandrasekaran, E. V.; Davidson, E. A. Glycosaminoglycans of normal and malignant cultured human mammary cells. *Cancer Res*. **1979**, *39*, 870-880.
2. Hennessey, P. T.; Hurst, R. E.; Hemstreet, G. P. 3rd, Cutter, G. Urinary glycosaminoglycan excretion as a biochemical marker in patients with bladder carcinoma. *Cancer Res*. **1981**, *41*, 3868-3873.
3. Lindahl, U.; Couchman, J.; Kimata, K.; Esko, J. D. Proteoglycans and Sulfated Glycosaminoglycans. In *Essentials of Glycobiology [Internet]*, 3rd edition; Varki, A., Cummings, R. D., Esko, J. D., Stanley, P., Hart, G. W., Aebi, M, Darvill, A. G., Kinoshita, T., Packer, N. H., Prestegard, J. H., Schnaar, R. L., Seeberger, P. H., editors; Cold Spring Harbor (NY): Cold Spring Harbor Laboratory Press, 2017; Ch. 17.
4. Afratis, N. A.; Nikitovic, D.; Multhaupt, H. A.; Theocharis, A. D.; Couchman, J. R.; Karamanos, N. K. Syndecans - key regulators of cell signaling and biological functions. *FEBS J.* **2017**, *284*, 27-41.
5. Iozzo, R. V.; Sanderson, R. D. Proteoglycans in cancer biology, tumour microenvironment and angiogenesis. *J. Cell. Mol. Med*. **2011**; *15*, 1013-1031.
6. Soares da Costa, D.; Reis, R. L.; Pashkuleva, I. Sulfation of glycosaminoglycans and its implications in human health and disorders. *Annu. Rev. Biomed. Eng*. **2017**, *19*, 1-26.
7. Kim, S. H.; Turnbull, J.; Guimond, S. Extracellular matrix and cell signalling: the dynamic cooperation of integrin, proteoglycan and growth factor receptor. *J. Endocrinol*. **2011**, *209*, 139-151.

8. Couchman, J. R.; Gopal, S.; Lim, H. C.; Nørgaard, S.; Multhaupt, H. A. Fell-Muir Lecture: Syndecans: from peripheral coreceptors to mainstream regulators of cell behavior. *Int*. *J*. *Exp*. *Pathol*. **2015**, *96*, 1-10.
9. Lim, H. C.; Multhaupt, H. A.; Couchman, J. R. Cell surface heparan sulfate proteoglycans control adhesion and invasion of breast carcinoma cells. *Mol*. *Cancer*. **2015**, *14*, 15.
10. Lindahl, U.; Li, J. P. Interactions between heparan sulfate and proteins-design and functional implications. *Int*. *Rev*. *Cell Mol*. *Biol*. **2009**, *276*, 105-159.
11. Gama, C. I.; Tully, S. E.; Sotogaku, N.; Clark, P. M.; Rawat, M.; Vaidehi, N.; Goddard, W. A. 3rd; Nishi, A.; Hsieh-Wilson, L. C. Sulfation patterns of glycosaminoglycans encode molecular recognition and activity. *Nat*. *Chem*. *Biol*. **2006**, *2*, 467-473.
12. Freire-de-Lima, L. Sweet and sour: the impact of differential glycosylation in cancer cells undergoing epithelial-mesenchymal transition. *Front*. *Oncol*. **2014**, *4*, 59.
13. Bracci, L.; Falciani, C.; Lelli, B.; Lozzi, L.; Runci, Y.; Pini, A.; De Montis, M. G.; Tagliamonte, A.; Neri, P. Synthetic peptides in the form of dendrimers become resistant to protease activity. *J*. *Biol*. *Chem*. **2003**, *278*, 46590-46595.
14. Falciani, C.; Lozzi, L.; Pini, A.; Corti, F.; Fabbrini, M.; Bernini, A.; Lelli, B.; Niccolai, N.; Bracci, L. Molecular basis of branched peptides resistance to enzyme proteolysis. *Chem*. *Biol*. *Drug Des*. **2007**, *69*, 216-221.
15. Falciani, C.; Fabbrini, M.; Pini, A.; Lozzi, L.; Lelli, B.; Pileri, S.; Brunetti, J.; Bindi, S.; Scali, S.; Bracci, L. Synthesis and biological activity of stable branched neurotensin peptides for tumor targeting. *Mol*. *Cancer Ther*. **2007**, *6*, 2441-2448.
16. Falciani, C.; Brunetti, J.; Pagliuca, C.; Menichetti, S.; Vitellozzi, L.; Lelli, B.; Pini, A.; Bracci, L. Design and in vitro evaluation of branched peptide conjugates: turning nonspecific cytotoxic drugs into tumor-selective agents. *ChemMedChem*. **2010**, *5*, 567-574.
17. Falciani, C.; Lelli, B.; Brunetti, J.; Pileri, S.; Cappelli, A.; Pini, A.; Pagliuca, C.; Ravenni, N.; Bencini, L.; Menichetti, S.; Moretti, R.; De Prizio, M.; Scatizzi, M.; Bracci, L. Modular branched

neurotensin peptides for tumor target tracing and receptor-mediated therapy: a proof-of-concept. *Curr*. *Cancer Drug Targets*. **2010**, *10*, 695-704.

18. Falciani, C.; Accardo, A.; Brunetti, J.; Tesauro, D.; Lelli, B.; Pini, A.; Bracci, L.; Morelli, G. Target-selective drug delivery through liposomes labeled with oligobranched neurotensin peptides. *ChemMedChem*. **2011**, *6*, 678-685.
19. Brunetti, J.; Falciani, C.; Lelli, B.; Minervini, A.; Ravenni, N.; Depau, L.; Siena, G.; Tenori, E.; Menichetti, S.; Pini, A.; Carini, M.; Bracci, L. Neurotensin branched peptide as a tumor-targeting agent for human bladder cancer. *Biomed Res. Int*. **2015**, *2015*, 173507.
20. Brunetti, J.; Riolo, G.; Gentile, M.; Bernini, A.; Paccagnini, E.; Falciani, C.; Lozzi, L.; Scali, S.; Depau, L.; Pini, A.; Lupetti, P.; Bracci, L. Near-infrared quantum dots labelled with a tumor selective tetrabranched peptide for in vivo imaging. *J*. *Nanobiotechnology*. **2018**, *16*, 21.
21. Depau, L.; Brunetti, J.; Falciani, C.; Scali, S.; Riolo, G.; Mandarini, E.; Pini, A.; Bracci, L. Coupling to a cancer-selective heparan-sulfate-targeted branched peptide can by-pass breast cancer cell resistance to methotrexate. *Oncotarget*. **2017**, *8*, 76141-76152.
22. Brunetti, J.; Pillozzi, S.; Falciani, C.; Depau, L.; Tenori, E.; Scali, S.; Lozzi, L.; Pini, A.; Arcangeli, A.; Menichetti, S.; Bracci, L. Tumor-selective peptide-carrier delivery of paclitaxel increases in vivo activity of the drug. *Sci*. *Rep*. **2015**, *5*, 17736.
23. Falciani, C.; Brunetti, J.; Lelli, B.; Ravenni, N.; Lozzi, L.; Depau, L.; Scali, S.; Bernini, A.; Pini, A.; Bracci, L. Cancer selectivity of tetrabranched neurotensin peptides is generated by simultaneous binding to sulfated glycosaminoglycans and protein receptors. *J*. *Med*. *Chem*. **2013**, *56*, 5009-5018.
24. Brunetti, J.; Depau, L.; Falciani, C.; Gentile, M.; Mandarini, E.; Riolo, G.; Lupetti, P.; Pini, A.; Bracci, L. Insights into the role of sulfated glycans in cancer cell adhesion and migration through use of branched peptide probe. *Sci*. *Rep*. **2016**, *6*, 27174.

25. Brunetti, J.; Riolo, G.; Depau, L.; Mandarini, E.; Bernini, A.; Karousou, E.; Passi, A.; Pini, A.; Bracci, L.; Falciani, C. Unraveling heparan sulfate proteoglycan binding motif for cancer cell selectivity. *Front*. *Oncol*. **2019**, *9*, 843.

26. Klingberg, F.; Chau, G.; Walraven, M.; Boo, S.; Koehler, A.; Chow, M. L.; Olsen, A. L.; Im, M.; Lodyga, M.; Wells, R. G.; White, E. S.; Hinz, B. The fibronectin ED-A domain enhances recruitment of latent TGF-β-binding protein-1 to the fibroblast matrix. *J. Cell Sci*. **2018**, *131,* jcs201293.

27. Midwood, K. S.; Valenick, L. V.; Hsia, H. C.; Schwarzbauer, J. E. Coregulation of fibronectin signaling and matrix contraction by Tenascin-C and Syndecan-4. *Mol*. *Biol*. *Cell*. **2004**, *15*, 5670-5677.

28. Moon, J. J.; Matsumoto, M.; Patel, S.; Lee, L.; Guan, J. L.; Li, S. Role of cell surface heparan sulfate proteoglycans in endothelial cell migration and mechanotransduction. *J. Cell*. *Physiol*. **2005**, *203*, 166-176.

29. Bass, M. D.; Roach, K. A.; Morgan, M. R.; Mostafavi-Pour, Z.; Schoen, T.; Muramatsu, T.; Mayer, U.; Ballestrem, C.; Spatz, J. P.; Humphries, M. J. Syndecan-4-dependent Rac1 regulation determines directional migration in response to the extracellular matrix. *J. Cell Biol*. **2007**, *177*, 527-538.

30. Suraneni, P.; Rubinstein, B.; Unruh, J. R.; Durnin, M.; Hanein, D.; Li, R. The Arp2/3 complex is required for lamellipodia extension and directional fibroblast cell migration. *J. Cell Biol*. **2012**, *197*, 239-251.

31. Suraneni, P.; Fogelson, B.; Rubinstein, B.; Noguera, P.; Volkmann, N.; Hanein, D.; Mogilner, A.; Li, R. A mechanism of leading-edge protrusion in the absence of Arp2/3 complex. *Mol*. *Biol*. *Cell*. **2015**, *26*, 901-912.

32. Steffen, A.; Koestler, S. A.; Rottner, K. Requirements for and consequences of Rac-dependent protrusion. *Eur*. *J. Cell Biol*. **2014**, *93*, 184-193.

33. Steffen, A.; Ladwein, M.; Dimchev, G. A.; Hein, A.; Schwenkmezger, L.; Arens, S.; Ladwein, K. I.; Margit Holleboom, J.; Schur, F.; Victor Small, J.; Schwarz, J.; Gerhard, R.; Faix, J.; Stradal, T. E.; Brakebusch, C.; Rottner, K. Rac function is crucial for cell migration but is not required for spreading and focal adhesion formation. *J. Cell Sci*. **2013**, *126*, 4572-4588.

34. Tai, Y. L.; Chen, L. C.; Shen, T. L. Emerging roles of focal adhesion kinase in cancer. *Biomed Res. Int*. **2015**, *2015*, 690690.

35. Coumans, J. V. F.; Davey, R. J.; Moens, P. D. J. Cofilin and profilin: partners in cancer aggressiveness. *Biophys. Rev*. **2018**, *10*, 1323-1335.

36. Ridley, A. J. Life at the leading edge. *Cell*. **2011**, *145*, 1012-1022.

37. Rotty, J. D.; Wu, C.; Bear, J. E. New insights into the regulation and cellular functions of the ARP2/3 complex. *Nat. Rev. Mol. Cell Biol*. **2013**, *14*, 7-12.

38. Mizuno, K. Signaling mechanisms and functional roles of cofilin phosphorylation and dephosphorylation. *Cell. Signal*. **2013**, *25*, 457-469.

39. Sidani, M.; Wessels, D.; Mouneimne, G.; Ghosh, M.; Goswami, S.; Sarmiento, C.; Wang, W.; Kuhl, S.; El-Sibai, M.; Backer, J. M.; Eddy, R.; Soll, D.; Condeelis, J. Cofilin determines the migration behavior and turning frequency of metastatic cancer cells. *J. Cell Biol*. **2007**, *179*, 777-791.

40. Collazo, J.; Zhu, B.; Larkin, S.; Martin, S. K.; Pu, H.; Horbinski, C.; Koochekpour, S.; Kyprianou, N. Cofilin drives cell-invasive and metastatic responses to TGF-β in prostate cancer. *Cancer Res*. **2014**, *74*, 2362-2373.

41. Suarez, C.; Kovar, D. R. Internetwork competition for monomers governs actin cytoskeleton organization. *Nat. Rev. Mol. Cell Biol*. **2016**, *17*, 799-810.

42. Döppler, H.; Storz, P. Regulation of VASP by phosphorylation: consequences for cell migration. *Cell Adh. Migr*. **2013**, *7*, 482-486.

43. Krause, M.; Gautreau, A. Steering cell migration: lamellipodium dynamics and the regulation of directional persistence. *Nat. Rev. Mol. Cell Biol*. **2014**, *15*, 577-590.

44. Ali, M.; Heyob, K.; Jacob, N. K.; Rogers, L. K. Alterative expression and localization of profilin 1/VASPpS157 and cofilin 1/VASPpS239 regulates metastatic growth and is modified by DHA supplementation. *Mol. Cancer Ther.* **2016**, *15*, 2220-2231.

45. Benz, P. M.; Blume, C.; Seifert, S.; Wilhelm, S.; Waschke, J.; Schuh, K.; Gertler, F.; Münzel, T.; Renné, T. Differential VASP phosphorylation controls remodeling of the actin cytoskeleton. *J. Cell Sci.* **2009**, *122*, 3954-3965.

46. Ponuwei, G. A. A glimpse of the ERM proteins. *J. Biomed. Sci.* **2016**, *23*, 35.

47. Haga, R. B.; Ridley, A. J. Rho GTPases: Regulation and roles in cancer cell biology. *Small GTPases*. **2016**, *7*, 207-221.

48. Lin, Y. L.; Lei, Y. T.; Hong, C. J.; Hsueh, Y. P. Syndecan-2 induces filopodia and dendritic spine formation via the neurofibromin-PKA-Ena/VASP pathway. *J. Cell Biol.* **2007**, *177*, 829-841.

49. Brühmann, S.; Ushakov, D. S.; Winterhoff, M.; Dickinson, R. B.; Curth, U.; Faix, J. Distinct VASP tetramers synergize in the processive elongation of individual actin filaments from clustered arrays. *Proc. Natl. Acad. Sci. U S A.* **2017**, *114*, E5815-E5824.

50. Breitsprecher, D.; Kiesewetter, A. K.; Linkner, J.; Urbanke, C.; Resch, G. P.; Small, J. V.; Faix, J. Clustering of VASP actively drives processive, WH2 domain-mediated actin filament elongation. *EMBO J.* **2008**, *27*, 2943-2954.